

Electronic Supplementary Information

Facile Signal-on Electrochemical DNA Sensing Platform for Ultrasensitive Detection of Pathogenic Bacteria Based on Exo III-assisted Autonomous Multiple-cycle Amplification

Qianqian Pei^a, Xiaolei Song^b, Su Liu^b, Jingfeng Wang^c, Xueqi Leng^b, Xuejun Cui^a, Jinghua Yu^a,

Yu Wang^{c}, Jiadong Huang^{a,c}*

a Key Laboratory of Chemical Sensing & Analysis in Universities of Shandong, college of Chemistry and Chemical Engineering, University of Jinan, Jinan 250022, P.R. China.

b School of Water Conservancy and Environment, University of Jinan, Jinan 250022, P.R. China.

c College of Biological Sciences and Technology, University of Jinan, Jinan 250022, P.R. China.

* Corresponding author. E-mail: bio_wangy@ujn.edu.cn; Tel.: +86-531-89736122; Fax: +86-531-82769122

Table S1. DNA Oligonucleotide sequences used in this work.

Oligonucleotide name	Sequence (5' to 3') description
Aptamer	AGTAATGCCCGGTAGTTATTCAAAGATGAGTAGGAAAAGA
Trigger	CCTACTCATCAAAAACGGGCATTACT
HAP1	CCACCAGCCCTACTCATCAAATAATTTTTTAGTAGGGCTGGTGG TTGATGAGTAGG
HAP2	SH-CTTCCTACTGAAG(MB)TAAAGATGAGTAGGGCTGGTGG
FQHP	(FAM)CCACCAGCCCTACTCATCAAATAATTTTTTAGTAGGGCTG GTGG(Dabcyl)TTGATGAGTAGG

Bacterial strains and growth conditions.

The cultured bacteria usually grow in a Luria-Bertani medium at 37 °C for 12 hours. The target bacteria were obtained by logarithmic growth and separated from the medium by centrifugation at 600 rpm for 5 minutes and then washed twice with phosphate-buffered saline (PBS) (10 mM, pH 7.4). The sediment was diluted with PBS to obtain a uniform cell suspension and the number of bacteria was determined by bacteria chamber.^{S1}

Preparation of the MCH/hairpin probe 2 (HAP2)/gold electrode.

The working gold electrode was first immersed in the piranha solution ($\text{H}_2\text{O}_2/\text{H}_2\text{SO}_4$, 1/3 in volume) for at least 30 minutes to dissolve impurities on the electrode surface, followed by cleaning thoroughly with ultrapure water. Then, prior to the manufacture of sensor, the working gold electrode was polished to a mirror-like surface on a fabric containing 0.3 and 0.05 μm alumina suspension and then ultrasonically cleaned in ethanol and ultrapure water, respectively. Finally, the electrode was again thoroughly rinsed with large amounts of ultrapure water and dried under a stream of nitrogen. The process of working electrode modification was as follows, 10 μL of 10 μM methylene blue (MB)-labelled hairpin probe 2 solution was added dropwise onto the surface of a clean gold electrode and incubated at 37 °C for 2 hours to obtain the HAP2/gold electrode. Afterwards, the obtained electrodes were washed using phosphate buffered saline (PBS) (10 mM, pH 7.4) to remove the HAP2 with weak adsorption on the electrode surface. Then, the electrodes were immersed into 2 mM MCH solution for 2 hours to block the unoccupied sites of the electrode surface and eliminate the effect of non-specific adsorption. Finally, the generating electrodes were rinsed with the water and named as the MCH/HAP2/Au electrode. In order to monitor the modification process of electrode, we confirmed the immobilization of each step of the electrode by measuring the EIS in 0.1 M KCl aqueous solution containing 5 mM $[\text{Fe}(\text{CN})_6]^{3-/4-}$. The frequency range was from 0.1 Hz to 100 kHz with 5 mV as the amplitude at a potential of 0.22 V (vs SCE).

Optimization of the experimental conditions.

To obtain the best analytical performance of this proposed biosensor, the concentrations of Exo III, HAP1, arched probe, and HAP2 were analyzed in detail by DPV measurements.

Since the concentration of Exo III significantly affected the amplification efficiency of the biosensor, it was very important to investigate the influence of Exo III concentration, and the results were shown in Figure S3A. As expected, it was observed that the current intensity increased with the increasing of the Exo III concentration and then reached a stable level at 10 U. Therefore, the optimal concentration of Exo III in the experiment is 10 U.

The concentrations of HAP1 and arched probe played the crucial part in signal amplification process of this strategy. The influences of HAP1 and arched probe concentrations were investigated by analyzing the current response of the biosensor towards the detection of 1.0×10^7 cfu mL⁻¹ target *S. typhimurium*. As shown in Figure S3B, it was found that the current intensity increased with increasing HAP1 concentration and remained unchanged between 10-20 μ M of the HAP1 concentration. Thus, the optimum concentration of HAP1 was selected as 10 μ M and used for all other measurements. Similarly, 1 μ M was selected as the optimal concentration of arched probe in the following experiments (Figure S3C).

It is also important for HAP2 concentration to achieve maximized current signal. High concentration of HAP2 could result in more folded structures, which produced the more significant change in current intensity. Whereas, it often generated higher background signal and lower sensitivity, which was not beneficial for the quantification of trace amounts of *S. typhimurium*. We analyzed the variances of the $(I-I_0)/I_0$ value with different HAP2 concentration, where I_0 and I are the current intensity of the electrochemical sensor at -0.22 V in the absence and presence of *S. typhimurium*, respectively. The analysis results were shown in Figure S3D, the $(I-I_0)/I_0$ value reached the maximum value at the HAP2 concentration of 10 μ M. Thus, the optimal concentration of HAP2 for electrode modification was 10 μ M.

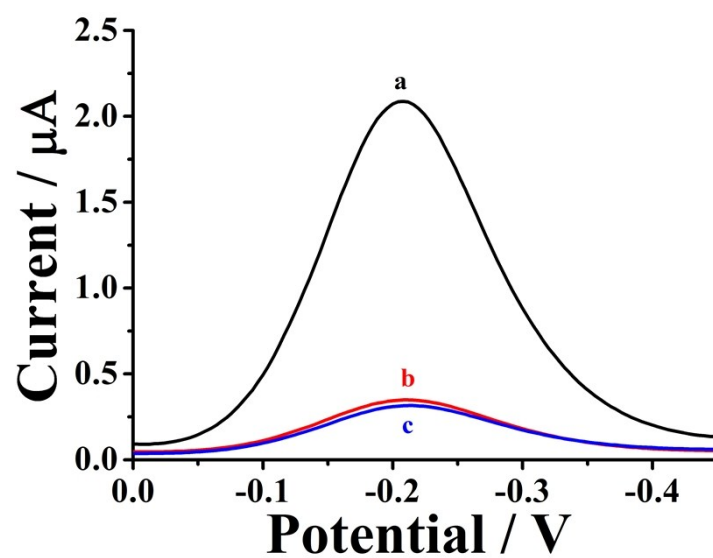


Figure S1. DPV responses of the biosensor obtained upon analyzing 1×10^7 cfu mL^{-1} live *S. typhimurium* (a), 1×10^7 cfu mL^{-1} heat-killed *S. typhimurium* (b), blank sample (c).

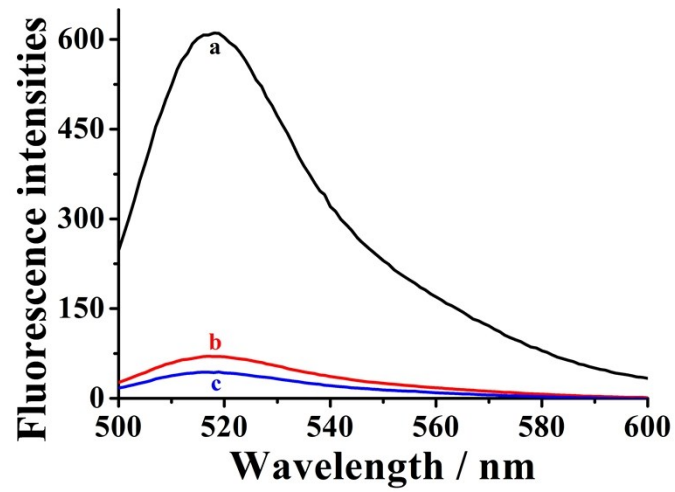


Figure S2. Fluorescence emission spectra responses for the Exo III-aided cyclic cleavage reaction. FQHP, arched probe, and Exo III in the presence of *S. typhimurium* (a), FQHP, arched probe, and Exo III in the absence of *S. typhimurium* (b), FQHP, arched probe and *S. typhimurium* in the absence of Exo III.

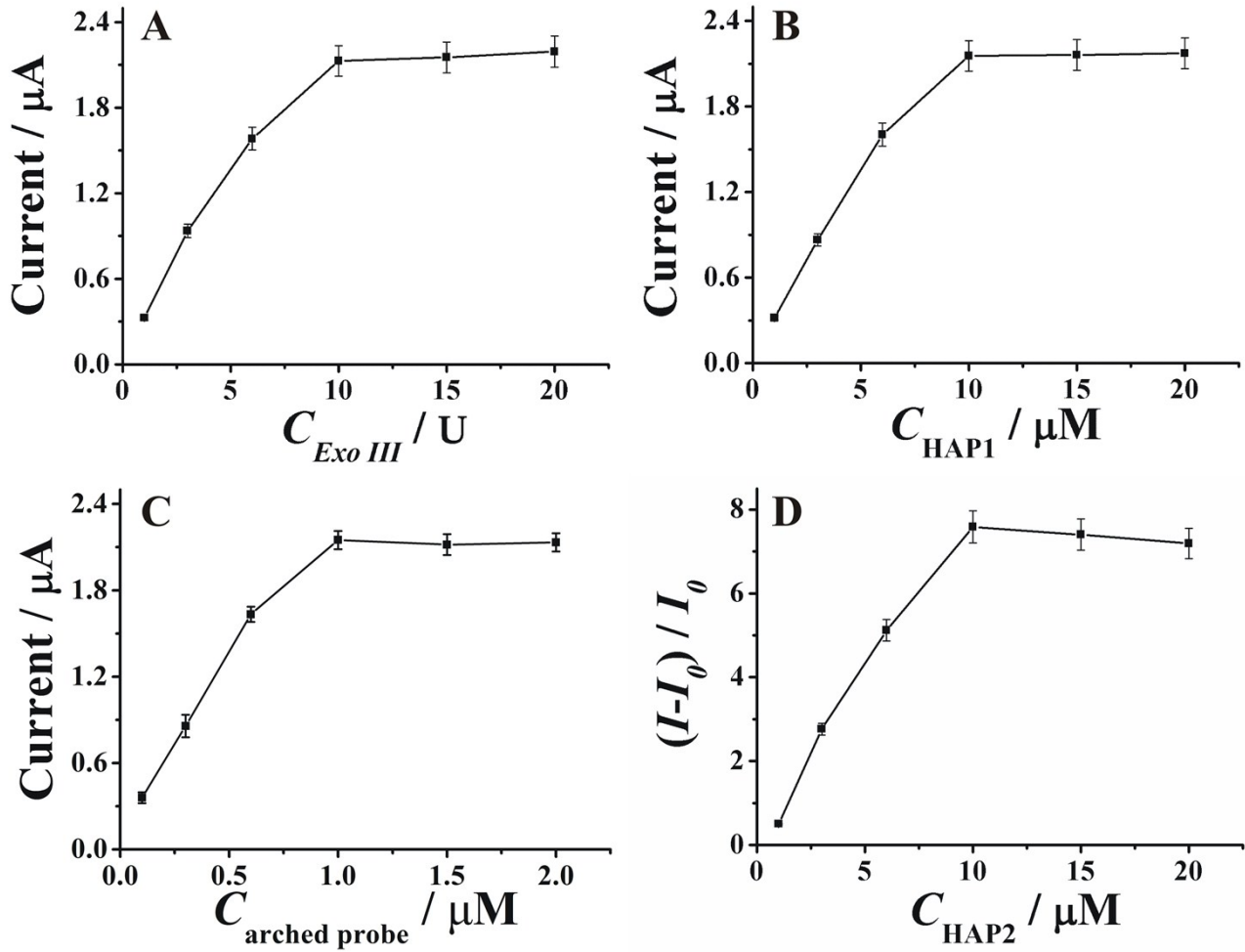


Figure S3. (A) Effect of the different concentrations of Exo III on the DPV signals of biosensor. (B) Effect of the different concentrations of HAP1 on the DPV signals of biosensor. (C) Effect of the different concentrations of arched probe on the DPV signals of biosensor. (D) Effect of the different concentrations of HAP2 on the DPV signals of biosensor.

Table S2. Comparison of different assay methods for pathogenic bacteria determination.

Detection methods	Detection range (cfu mL ⁻¹)	Detection limit (cfu mL ⁻¹)	Detection Time (h)	Reference
Enzyme-linked immunosorbent assay (ELISA)	8×10^1 - 8×10^8	8×10^1	4.5	[S2]
Quartz crystal microbalance (QCM)	1×10^2 - 4×10^4	1×10^2	1.5	[S3]
Surface plasmon resonance (SPR)	2×10^1 - 1×10^2	2×10^1	10	[S4]
Colorimetric immunoassay	8.4×10^3 - 8.4×10^7	1.70×10^3	1.5	[S5]
Fluorescence	1×10^1 - 1×10^6	9.86×10^0	2	[S6]
Electrochemical	6×10^2 - 6×10^6	6×10^2	4.5	[S7]
Electrochemical	1×10^1 - 1×10^7	8×10^0	4	This work

Table S3. *S. typhimurium* detection in real samples.

Samples	Spiked amount (cfu mL ⁻¹)	Our method (cfu mL ⁻¹)	Recovery (%)	Plate count method (cfu mL ⁻¹)
Milk	1.0×10 ¹	(1.019±0.022)×10 ¹	101.9	1.013×10 ¹
	1.0×10 ²	(1.022±0.014)×10 ²	102.2	0.967×10 ²
	1.0×10 ³	(0.957±0.028)×10 ³	95.7	0.972×10 ³
	1.0×10 ⁴	(0.964±0.042)×10 ⁴	96.4	1.036×10 ⁴
	1.0×10 ⁵	(1.025±0.038)×10 ⁵	102.5	0.969×10 ⁵

References

- S1. T. Qiu, Y. Wang, J. Yu, S. Liu, H. Wang, Y. Guo, and J. Huang, *Rsc Adv.*, 2016, **6**, 62031-62037.
- S2. R. Chen, X. Huang, H. Xu, Y. Xiong, Y. Li, *ACS Appl. Mater. Inter.*, 2015, **7**, 28632-28639.
- S3. V. C. Ozalp, G. Bayramoglu, Z. Erdem, and M. Y. Arica, *Anal. Chim. Acta*, 2015, **853**, 533-540.
- S4. E. Bulard, A. Bouchet-Spinelli, P. Chaud, A. Roget, R. Calemczuk, S. Fort, T. Livache, *Anal. Chem.*, 2015, **87**, 1804-1811.
- S5. H. Zhu, G. Zhao, S. Q. Wang, W. Dou, *Microchim. Acta*, 2017, **184**, 1873-1880.
- S6. X. Q. Leng, Y. Wang, S. Liu, Q. Q. Pei, X. J. Cui, Y. Q. Tu, X. J. Liu, J. D. Huang, *Sensor. Actuat. B-Chem.*, 2017, **252**, 689-696.
- S7. X. Wang, P. Zhu, F. Pi, H. Jiang, J. Shao, Y. Zhang, X. Sun, *Biosens. Bioelectron.*, 2016, **81**, 349-357.